Electronic Supplementary Material (ESI)

Itaconate is a covalent inhibitor of the *Mycobacterium tuberculosis* isocitrate lyase

Brooke X. C. Kwai, Annabelle J. Collins, Martin J. Middleditch, Jonathan Sperry, Ghader Bashiri and Ivanhoe K. H. Leung

Materials and Methods

Protein expression and purification: Wild-type ICL1 was cloned into pNIC28-Bsa4, expressing the protein with an N-terminal polyhistidine tag and a tobacco etch virus (TEV) protease cleavage site. The plasmid encoding N-terminal polyhistidine-tagged C191S ICL1 along with a thrombin cleavage site (pET-28a(+), Table S1) was purchased from GenScript. Expression and purification of the wild-type and C191S ICL1 followed the procedure as describe previously in Bhusal *et al*.[1] In brief, recombinant plasmids encoding wild-type and C191S ICL1 were transformed into *Escherichia coli* BL21 (DE3) using heat shock. A single transformed colony was used to inoculate 2YT media with 50 μg/mL of kanamycin, shaking at 37 °C for 12 hours. The starter culture was then diluted 1:100 in fresh 2YT media, which was then grown with 50 μg/mL of kanamycin at 37 °C until reaching OD ~0.6. The culture was induced with 0.2 mM isopropyl β-D-1-thiogalactopyranoside (IPTG) then further grown at 18 °C for 16 to 18 hours, followed by harvesting the cells by centrifugation by using a Sorvall Lynx 4000 centrifuge (Thermo Scientific) at 3600 × g at 4 °C. Cells were lysed on ice by sonication (4 × 20 seconds) burst at 60% amplitude with 40 seconds rest in between. Protein purification was performed at 4°C. It was first purified by immobilised metal affinity chromatography using a 5 mL HisTrap column (GE Healthcare) followed by size exclusion chromatography (GE Healthcare). The protein was eluted in 50 mM HEPES, 500 mM NaCl, pH 7.5 and was then aliquoted and stored at -80 °C until needed. The polyhistidine tag was not cleaved from the proteins in this study.

Production and purification of ICL2 followed the procedure previously described in Bhusal *et al*.[2] In brief, the recombinant plasmid (pYUB28b-*icl2*) was cotransformed with pGro7 plasmid in *E. coli* BL21 (DE3) LOBSTR cells. The inoculated TB media containing 50 μg/mL of hygromycin and chloramphenicol was incubated at 37 °C until OD reached ~0.5. L-Arabinose was then added to a final concentration of 0.1% *w/v*. Cells were harvested by

centrifugation after another 16 hours of incubation at 37 °C. Cells were lysed on ice by sonication (4 × 20 seconds) burst at 60% amplitude with 40 seconds rest in between. Protein purification was performed at 4 °C. It was first purified by immobilised metal affinity chromatography using a 5 mL HisTrap column (GE Healthcare) followed by size exclusion chromatography (GE Healthcare). The protein was eluted in 20 mM HEPES, 150 mM NaCl, 1 mM β-mercaptoethanol, pH 7.5 and was then aliquoted and stored at -80 °C until needed. The polyhistidine tag was not cleaved from the proteins in this study.

Co-crystallisation of ICL1 proteins with itaconate: Purified ICL1 was concentrated to 19 mg/mL, incubated with 1 mM itaconate and 5 mM $MgCl_2$ on ice for 4 hours. Initial screening were performed by sitting drop vapour diffusion, using commercial screens JCSG-*plus*, Morpheus and PACT *premier*. Crystallisation screens were dispensed by an Oryx4 robot (Douglas Instruments) onto 96- well vapour diffusion plates (Intelliplate, Art Robbins Instrument) at 18 °C. Drop size was set to 1 µL of reservoir solution and 1 µL of the protein solution. The best diffracting crystal (needle shaped, 3 mm) was obtained from a PACT condition containing of 20% *w*/*v* PEG 3350, 0.2 M sodium formate and 0.1 M bis-tris propane at pH 7.5. For data collection, protein crystals were cryo-cooled in liquid nitrogen, with no additional cryoprotectant. Although a previous study[3] has concluded that at least 35% *w/v* PEG3350 is needed to act as an intrinsic cryoprotectant, in our study the presence of 20% *w/v* PEG3350 was observed to be sufficient to provide cryoprotection at cryogenic temperature. A similar procedure was used to crystallise C191S ICL1. The protein (15 mg/mL) was incubated with 1 mM itaconate, glyoxylate and 5 mM $MgCl_2$. Crystal was also fetched from a PACT condition with 20% *w*/*v* PEG 3350 and 0.2 M sodium fluoride with 20% *v*/v glycerol in mother liquid as cryoprotection.

Data collection and processing: Diffraction data were collected at the Australian Synchrotron MX2 beamline.[4] Diffraction images were processed using XDS,[5] and scaled with

AIMLESS[6] from the CCP4i programme suite. The structure was solved by molecular replacement using Phaser[7] with the existing *Mtb* ICL1 structure (PDB 1F8I)[8] as a search model. The structure was completed by cycles of manual building using COOT[9] and refined using REFMAC5.[10] Full data collection statistics are shown in Table S2. The cysteine-bound itaconate was built in Coot's ligand builder, Lidia,[11] and a topology file was generated using PRODRG.[12] The PDB_REDO programme[13] was used in the final stages of refinement, and the final structure was assessed with the Molprobity.[14] All refinement statistics are summarised in Table S3.

Tandem mass spectrometry: Protease digestion was performed to confirm the itaconate binding site and the identity of the covalent adduct formed. ICL1/ICL2 samples (20 µM) were incubated with excess itaconate (1 mM) in the presence of Mg^{2+} (5 mM) overnight on ice to ensure complete adduct formation. The samples were run on SDS-PAGE, and the protein gel band was excised and destained with 50% *v/v* acetonitrile in 50 mM ammonium bicarbonate. The samples were then reduced by heating with 10 mM DTT at 56 °C for 15 mins and alkylated by incubation with 50 mM iodoacetamide in the dark for 30 mins. Trypsin protease (12.5 ng/µL in 25 mM ammonium bicarbonate) was added to cover the dehydrated gel band pieces, which were digested in a microwave at 45 °C for 1 hour. The resulting peptides were diluted 50-fold in 0.1% *v/v* formic acid and analysed by LC-MS/MS. Samples were injected onto a 0.3x 10 mm trap column packed with Reprosil C18 media (Dr Maisch) and desalted for 5 minutes at 10 µL/min before being separated on a 0.075 x 200 mm picofrit column (New Objective) packed in-house with Reprosil C18 media. The following gradient was applied at 300nL/min using a NanoLC 400 UPLC system (Eksigent): 0 min 5% *v/v* B; 18 min 50% *v/v* B; 20 min 98% *v/v* B; 22 min 98% *v/v* B; 23 min 5% *v/v* B; 30 min 5% *v/v* B where A was 0.1% *v/v* formic acid in water and B was 0.1% *v/v* formic acid in acetonitrile. The picofrit spray was directed into a TripleTOF 6600 Quadrupole-Time-of-Flight mass spectrometer (Sciex) scanning from

350-2000 m/z for 250ms, followed by 35 ms MS/MS scans on the 30 most abundant multiply-charged peptides (m/z 80-1600) for a total cycle time of ~1.3 seconds. The mass spectrometer and HPLC system were under the control of the Analyst TF 1.7 software package (Sciex). A custom definition for itaconate was added to the set of available modifications in ProteinPilot v5.0 (Sciex) The peptides containing the modified active site cysteine residue were identified from a search of the data against a protein sequence database containing the ICL entries.

LC-MS: The covalent binding of itaconate and the rate of covalent modification was measured by LC-MS using a QSTAR XL electrospray quadrupole time-of-flight system (Sciex) with a C4 HPLC column attached. The LC step helped to clean up any residual buffer and salt that might cause signal interference and contamination. All experiments were carried out in positive ionisation mode after calibration with renin standard (Sciex). 10 µL of diluted sample was injected and eluted with a linear gradient of 25% *v/v* A (0.1% *v/v* formic acid) to 65% *v/v* B (0.1% *v/v* formic acid in acetonitrile) formed at 6ul/min over 30 mins. A TOF-MS scan from m/z 600- 2000 was performed. The raw data was deconvoluted using the Reconstruct Protein tool in PeakView v2.2 (Sciex) to obtain the intact protein mass for ligand binding, and the peak heights for comparison.

For covalent binding studies, 20 µM of protein was mixed with 1 mM ligand (itaconate or glyoxylate) in the presence or absence of 5 mM $MgCl_2$. The mixture was left on ice for 12 hours to ensure complete reaction. Sample was diluted 200-fold with 0.1% *v/v* formic acid just prior to injection to LC-MS.

For the monitoring of covalent adduct formation over time, the reaction was started by adding 1 mM ligand and 5 mM $MgCl_2$ into 20 µM of ICL1. 2 µL of the reaction mixture was taken out at specific time points, the reaction was stopped by diluting 100-fold in 0.1% *v/v* formic acid and flash freezing with liquid nitrogen. Samples were thawed just prior to injection for

LC-MS analysis. Peak heights of modified and unmodified protein samples were compared as ratios in order to monitor the degree of covalent modification over time.

UV-Vis inhibition assay: The phenylhydrazine-based kinetic assay was optimised based on Pham *et al.*[15] Experiments were carried out on transparent 96-well plates (Thermo Scientific). 20 nM of ICL1 were pre-incubated with 1 mM $MgCl_2$, and varying concentration of itaconate or itaconate analogues in 50 mM Tris (pH 7.5) for an hour at room temperature. The reaction was initiated by adding 1 mM DL-isocitrate and 10 mM phenylhydrazine-HCl. The ICL enzymatic product glyoxylate reacts with phenylhyrazine-HCl to form phenylhydrazone. The formation of phenylhydrazone was measured spectrophotometrically ($\varepsilon_{324} = 17{,}000\ M^{-1}\ cm^{-1}$) by a Perkin Elmer EnSpire Multimode Reader every 30 seconds for 25 minutes. The initial rate of the reaction was plotted against inhibitor concentration, and the data was fitted by nonlinear regression using the "Sigmoid, 3 Parameter" model using SigmaPlot 14.0 (Systat Software) to determine the IC_{50} value.

NMR binding assay: NMR experiments were conducted at a ^1H frequency of 500 MHz using a Bruker Avance III HD spectrometer equipped with a 5 mm Prodigy BB/^{1}H&F Cryoprobe. All experiments were conducted at 298 K. Sampled are buffered using 50 mM Tris-D11 at pH 7.5 in 90% H_2O and 10% D_2O. Water suppression was achieved using the excitation sculpting method. For binding constant (K_D) determination, varying concentrations of ICL1 was titrated into 20 μM itaconate, and (where applicable) 2 mM glyoxylate and/or 5 mM $MgCl_2$. The binding affinity was measured through the decrease in free itaconate peak height. The ratio of the NMR peak height of itaconate was plotted against protein concentration and fitted by a nonlinear regression one site saturation binding model $y = Bmax * \frac{[ICL]}{(KD+[ICL])}$ using SigmaPlot 14.0 (Systat Software).

Itaconate analogue synthesis: Itaconic acid was purchased from Sigma-Aldrich. Dimethyl itaconate (**1**) was synthesised according to Malferrari *et al.*[15] Dimethyl-2-ethylidenesuccinate

(**2**) was synthesised according to Ballini *et al.*[16] 2-Benzylidenesuccinic acid (**3**) was synthesised according to Wang *et al.*[17] 2-Ethylidenebutanedioic acid (**4**) was synthesised according to Ballini *et al*[18] with some modifications. Trans-aconitic acid (**5**) and cis-aconitic acid (**6**) were obtained from AK Scientific.

Supplementary Figures

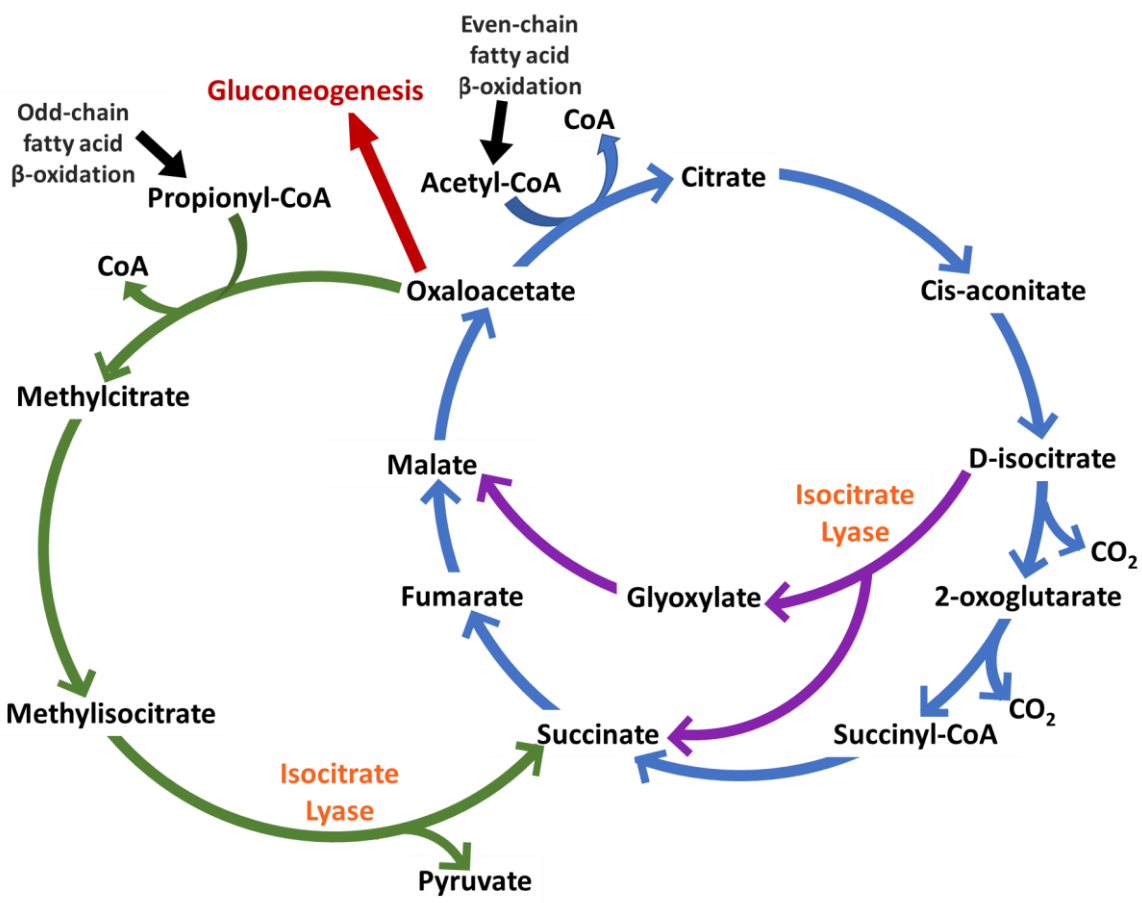

Figure S1: In *Mtb*, ICL isoforms 1 and 2 are involved in both the glyoxylate shunt (purple) and the methylcitrate cycle (green). In the glyoxylate shunt, ICLs catalyse the conversion of D-isocitrate to glyoxylate and succinate, enabling the bacteria to bypass the tricarboxylic acid cycle (blue) to preserve carbon for gluconeogenesis. In the methylcitrate cycle, ICLs catalyse the conversion of methylisocitrate to pyruvate and succinate as part of the detoxification pathway when odd-chain fatty acids were used as energy source.[20]

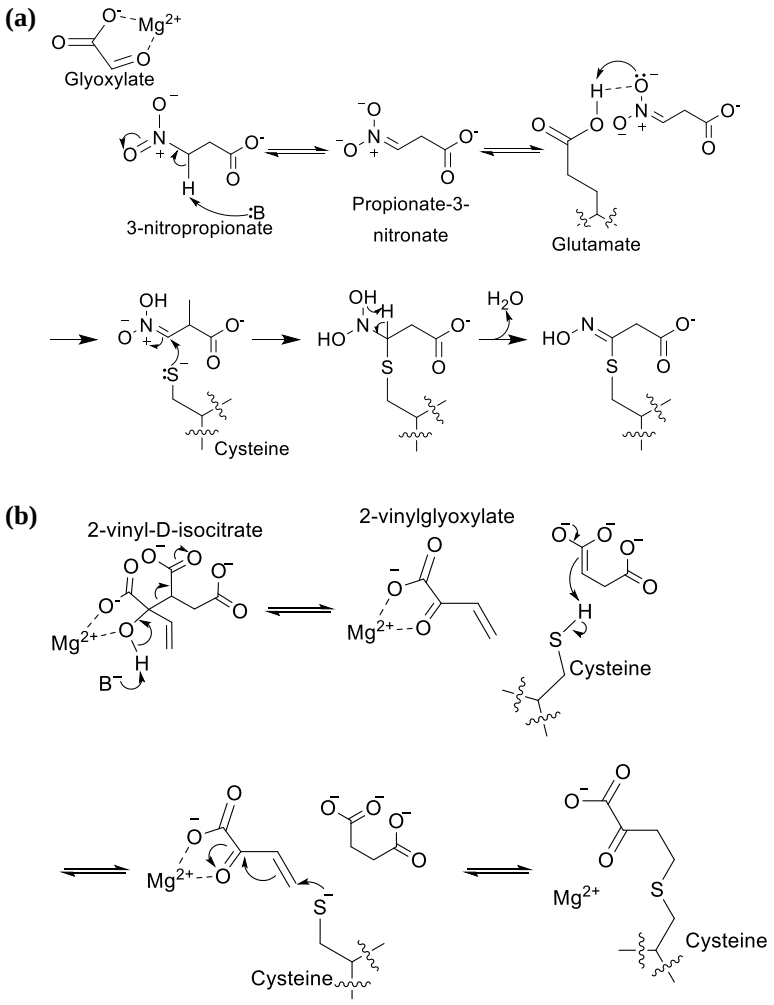

Figure S2: Previous studies found that the catalytic cysteine residue of the ICL1 (Cys191) may react with Michael acceptors to form covalent adducts. **(a)** In the case of 3-nitropropionate,[21] the Michael acceptor was propionate-3-nitronate (formed by the deprotonation of 3-nitropropionate), and **(b)** in the case of 2-vinyl-D-isocitrate,[15] the Michael acceptor was 2-vinylglyoxylate, which was formed as a result of the ICL-catalysed lysis of 2-vinyl-D-isocitrate.

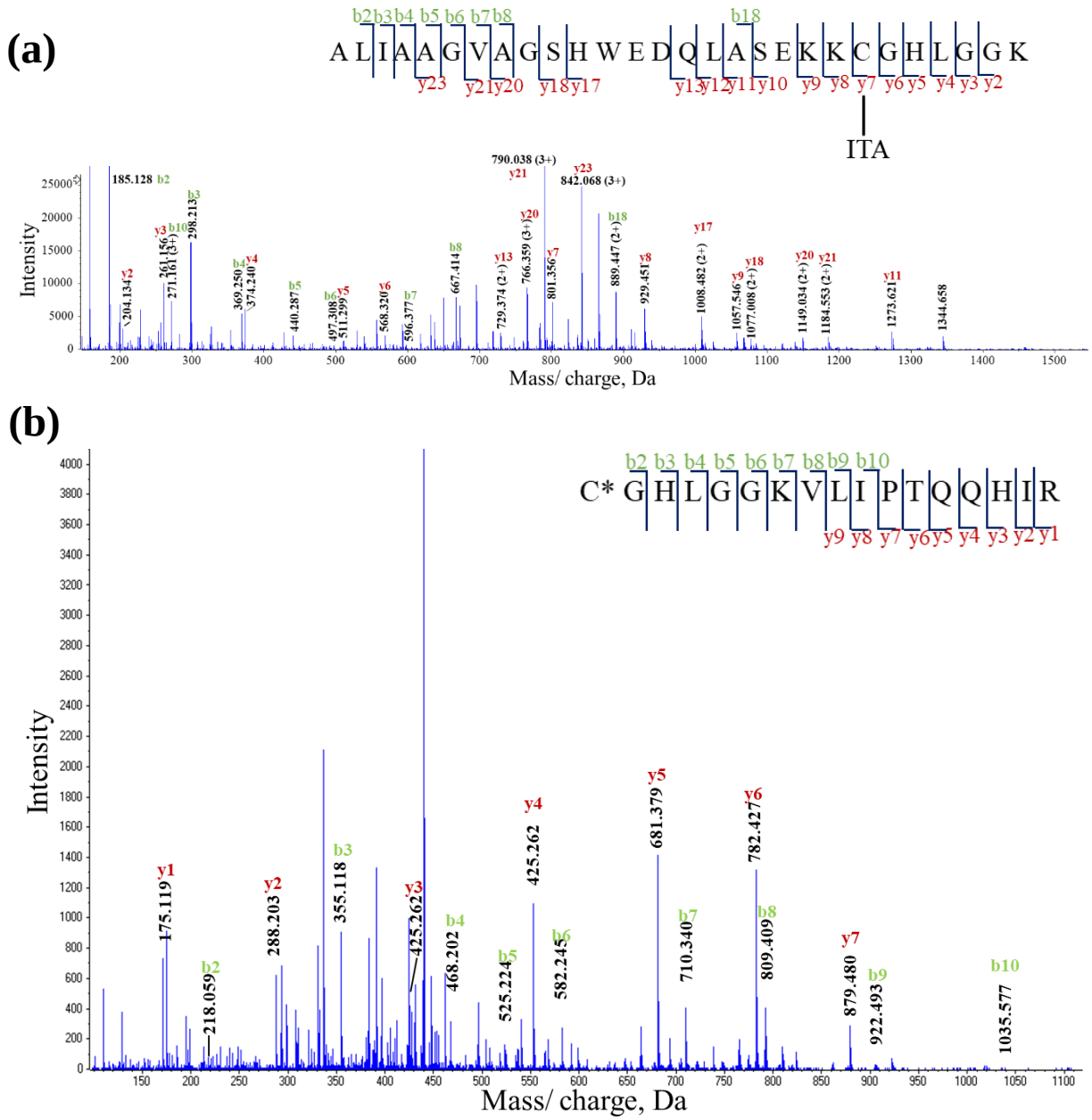

Figure S3: (a) LC-MS/MS spectrum of trypsin-digested ICL1 pre-incubated with itaconate and Mg^{2+}. The proteolytic peptide Ala170-Lys197 showed a m/z of 593.49^{5+}, which corresponds to an observed molecular weight of 2962.5 Da. The calculated molecular weight of the peptide is 2832.4 Da. The differences in calculated and observed molecular weight is 130 Da, which matches the presence of an itaconate covalent modification. **(b)** LC-MS/MS spectrum of trypsin-digested ICL1 without itaconate as a negative control. The proteolytic peptide Cys191-Arg207 showed a m/z of 383.6^{5+}, which corresponds to an observed molecular

weight of 1913 Da. The calculated molecular weight of the peptide is 1913 Da. The asterisk indicates the cysteine was carbamidomethylated. When fragment ions are not singly charged, their charge states are indicated in bracket.

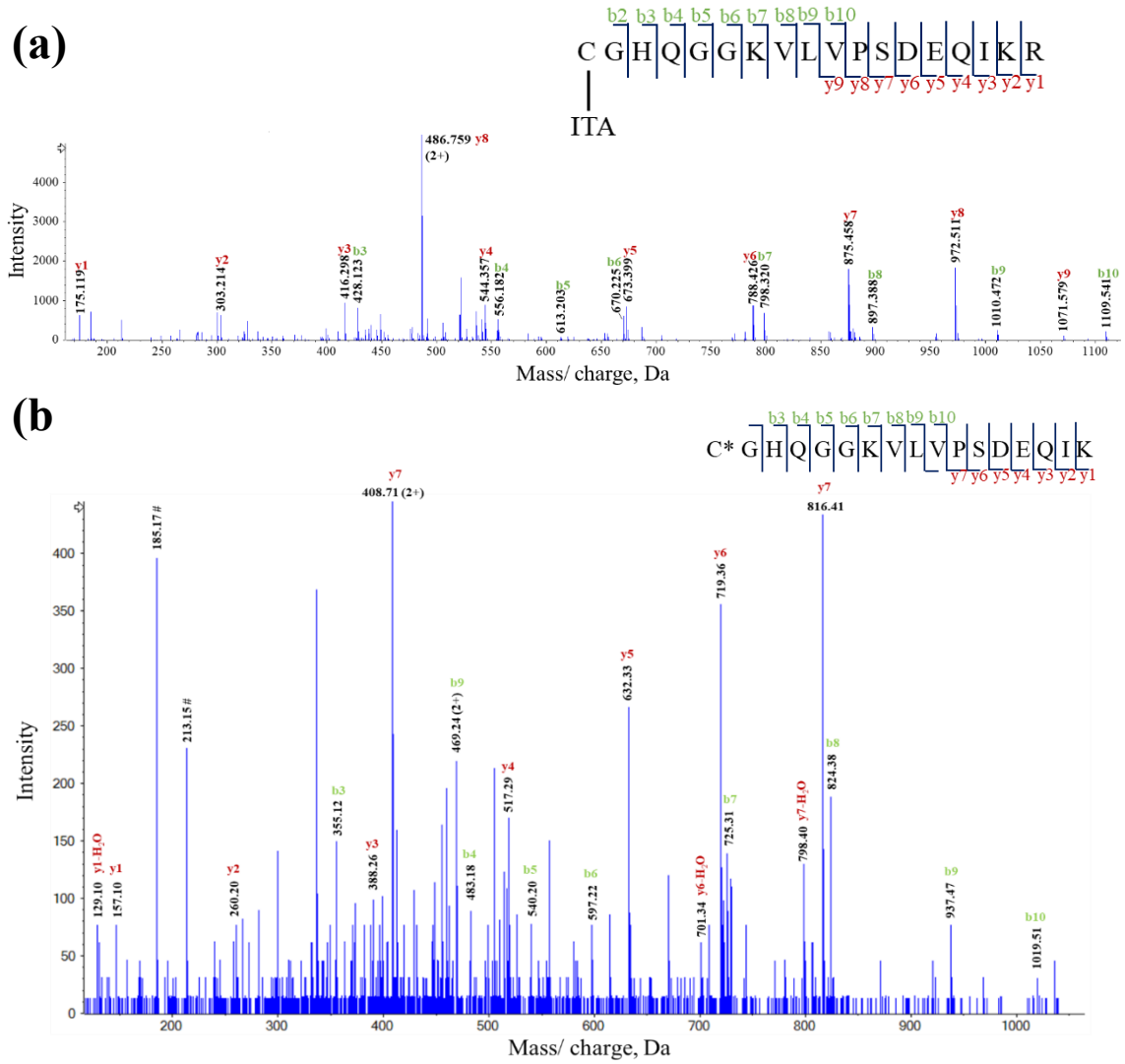

Figure S4: (a) LC-MS/MS spectrum of trypsin-digested ICL2 pre-incubated with itaconate and Mg^{2+}. The proteolytic peptide Cys215-Arg232 showed a m/z of 521.0^{4+}, which corresponds to an observed molecular weight of 2080 Da. The calculated molecular weight of the peptide is 1951 Da. The differences in calculated and observed molecular weight is 131 Da, which matches the presence of an itaconate covalent modification. **(b)** LC-MS/MS spectrum of trypsin-digested ICL1 without itaconate as a negative control. The proteolytic peptide Cys215-Lys231 showed a m/z of 463.7^{4+}, which corresponds to an observed molecular weight of 1850 Da. The calculated molecular weight of the peptide is 1851 Da. The asterisk indicates the cysteine was carbamidomethylated. The prominent fragment ion with m/z 213.15 (indicated by hashtag) is an internal ion with the composition Leu+Val (LV or VL). The ion with m/z

185.17 is the same species minus CO (i.e. the “a-type ion” for this internal ion). When fragment ions are not singly charged, their charge states are indicated in bracket.

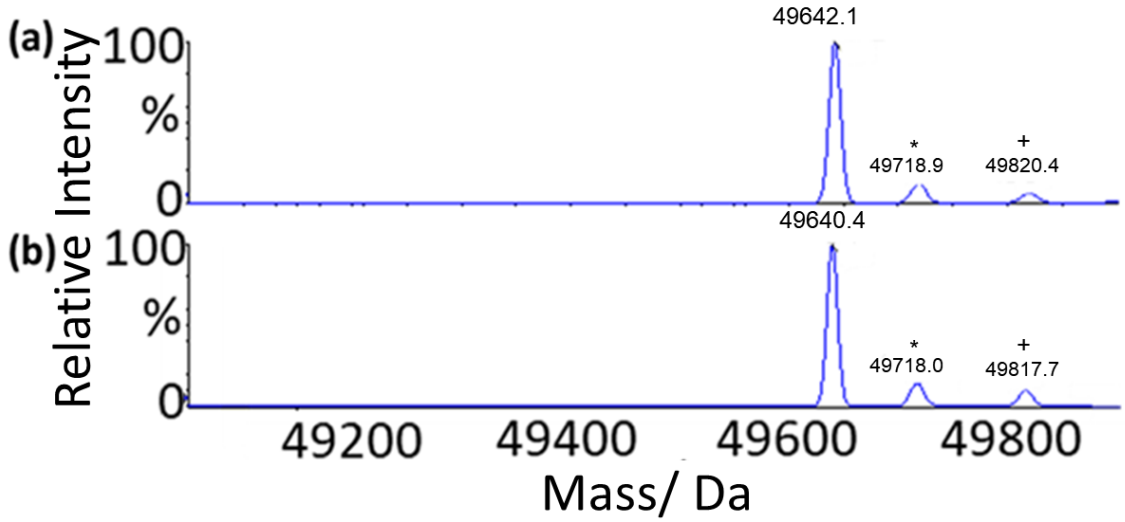

Figure S5: LC-MS analysis of wildtype ICL1. **(a)** Mass spectrum of wildtype ICL1. The calculated molecular weight of wildtype ICL1 is 49639.3 Da (observed: 49642.1 Da). **(b)** Mass spectrum of wildtype ICL1 pre-incubated with itaconate in the absence of Mg^{2+}. * and $^{+}$ denote the phosphoryl and gluconate adducts of ICL1, which are formed by gluconoylation during protein expression.[22]

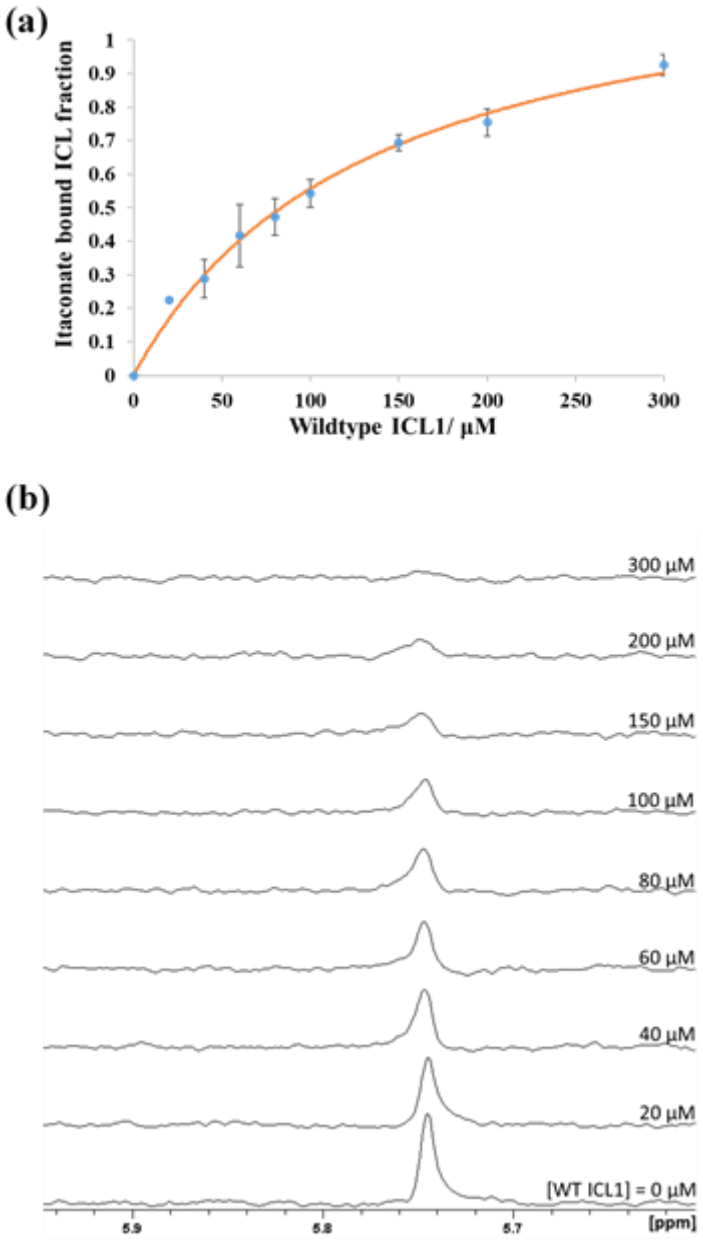

Figure S6: (a) Binding of itaconate to wildtype ICL1 in presence of Mg^{2+}. The K_D value was found to be 112 ± 10.7 µM. Error bars represent standard deviations from three individual experiments. **(b)** Corresponding ^1H NMR spectra. K_D measured at a fixed itaconate concentration (20 µM) and varying ICL1 concentration (0 to 300 µM). The Mg^{2+} concentration was 5 mM. Itaconate binding was monitored via the decrease of the itaconate alkene $=CH_2$ peak at 5.75 ppm as a function of protein concentration.

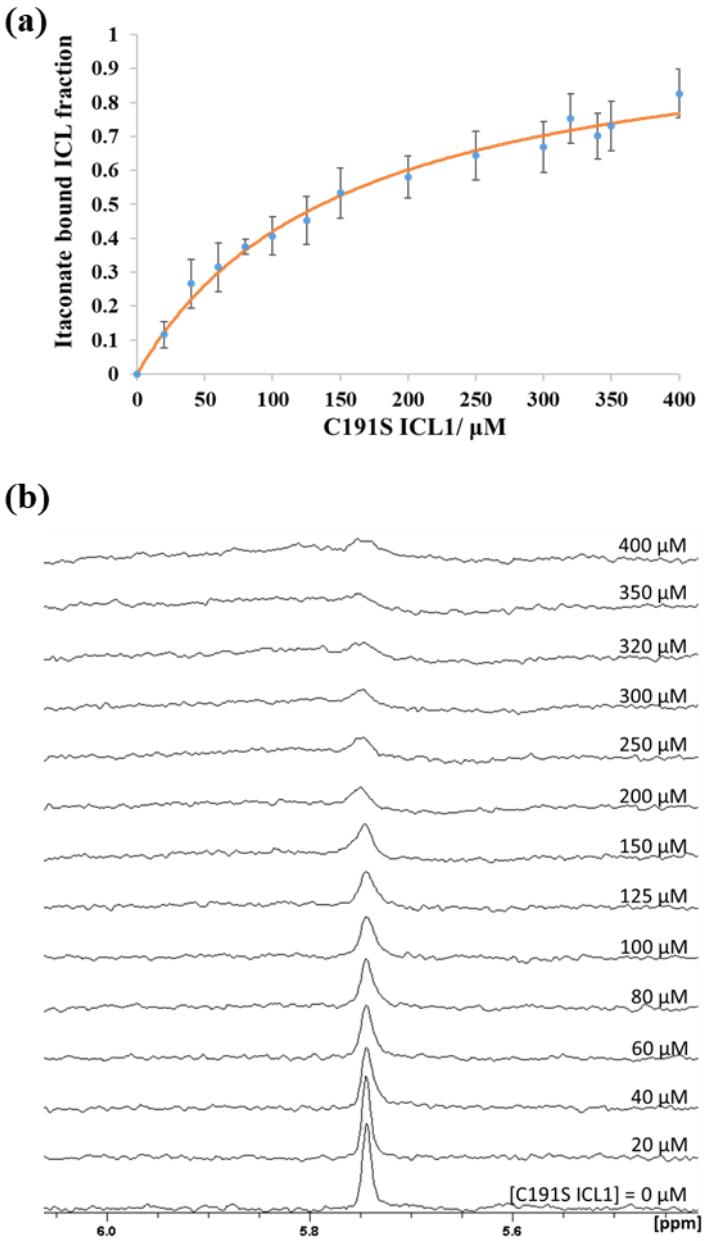

Figure S7: (a) Binding of itaconate to C191S ICL1 in presence of Mg^{2+}. The K_D value was found to be 155 ± 29.4 µM. Error bars represent standard deviations from three individual experiments. **(b)** Corresponding ^1H NMR spectra. K_D measured at a fixed itaconate concentration (20 µM) and varying C191S ICL1 concentration (0 to 400 µM). The Mg^{2+} concentration was 5 mM. Itaconate binding was monitored via the decrease of the itaconate alkene $=CH_2$ peak at 5.75 ppm as a function of protein concentration.

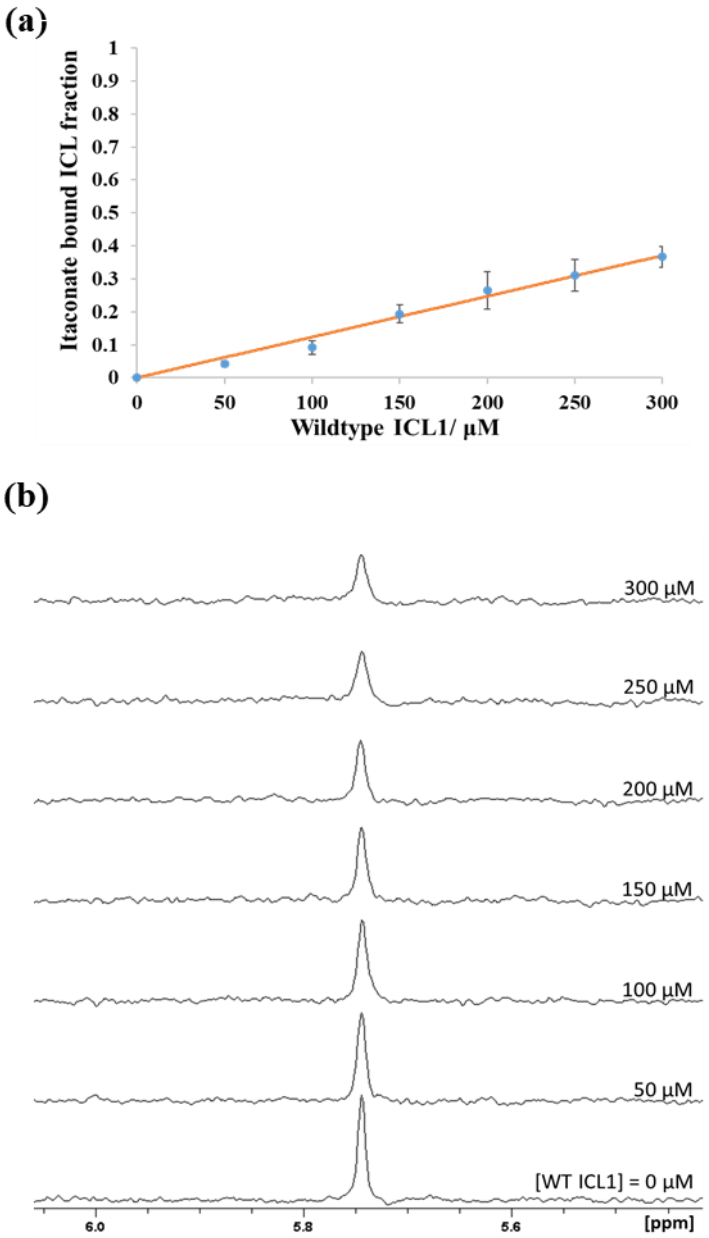

Figure S8: (a) Binding of itaconate to wildtype ICL1 in absence of Mg^{2+}. The K_D value was found to be >>500 µM. Error bars represent standard deviations from three individual experiments. **(b)** Corresponding ^1H NMR spectra. K_D measured at a fixed itaconate concentration (20 µM) and varying ICL1 concentration (0 to 300 µM). Itaconate binding was monitored via the decrease of the itaconate alkene $=CH_2$ peak at 5.75 ppm as a function of protein concentration.

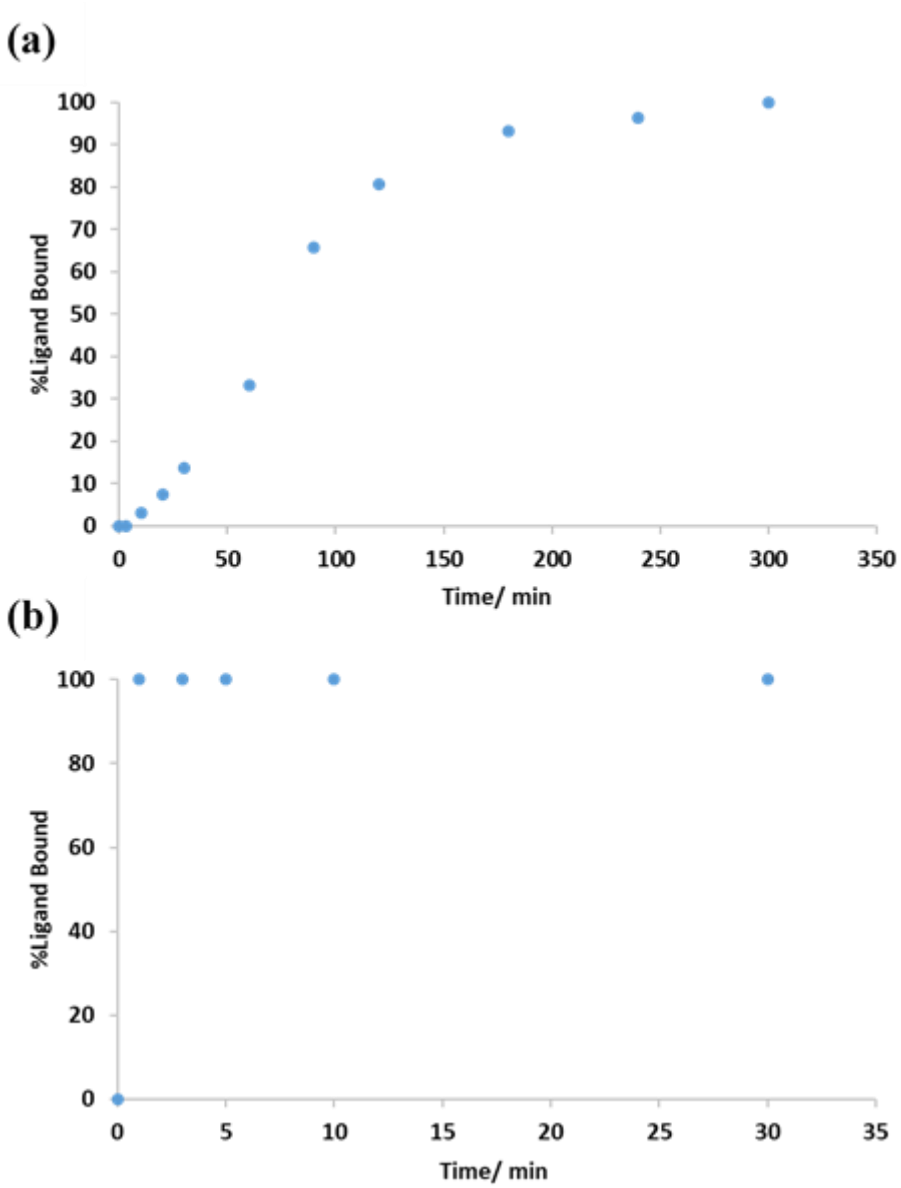

Figure S9: Comparison between the rate of ICL1 covalent modification **(a)** in the absence and **(b)** in the presence of glyoxylate. The reaction was initiated by adding 20 µM of ICL1 into a mixture of 5 mM $MgCl_2$, 1 mM itaconate and 1 mM glyoxylate (where applicable) in 50 mM Tris pH 7.5 on ice. 2 µL of the reaction mixture was taken out at specific time points, the reaction was stopped by diluting the mixture 100-fold in 0.1% *v/v* formic acid and flash freezing with liquid nitrogen. Samples were thawed just prior to injection for LC/MS analyses. Deconvoluted peak heights of modified and unmodified protein samples were compared in order to determine the degree of covalent modification over time.

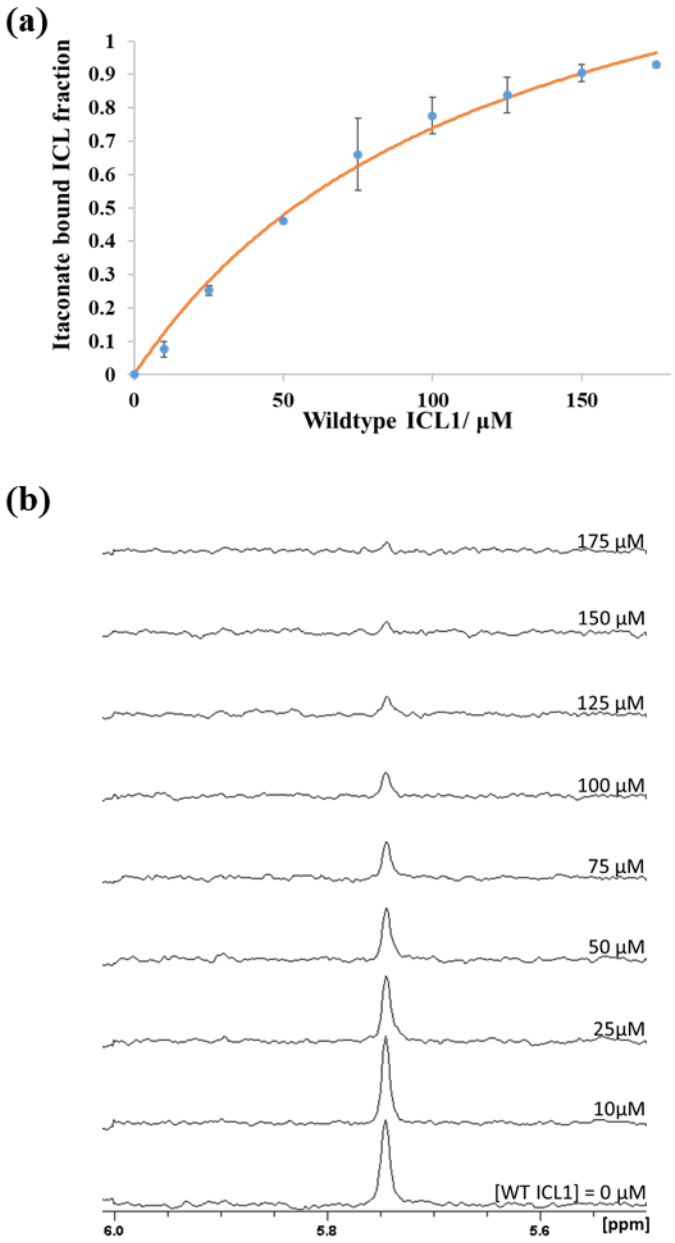

Figure S10: (a) Binding of itaconate to wildtype ICL1 in presence of Mg^{2+} and glyoxylate. The K_D value was found to be 123 ± 18.0 µM. Error bars represent standard deviations from three individual experiments. **(b)** Corresponding ^1H NMR spectra. K_D measured at a fixed itaconate concentration (20 µM) and varying ICL1 concentration (0 to 175 µM). The Mg^{2+} concentration was 5 mM and the glyoxylate concentration was 2 mM. Itaconate binding was monitored via the decrease of the itaconate alkene $=CH_2$ peak at 5.75 ppm as a function of protein concentration.

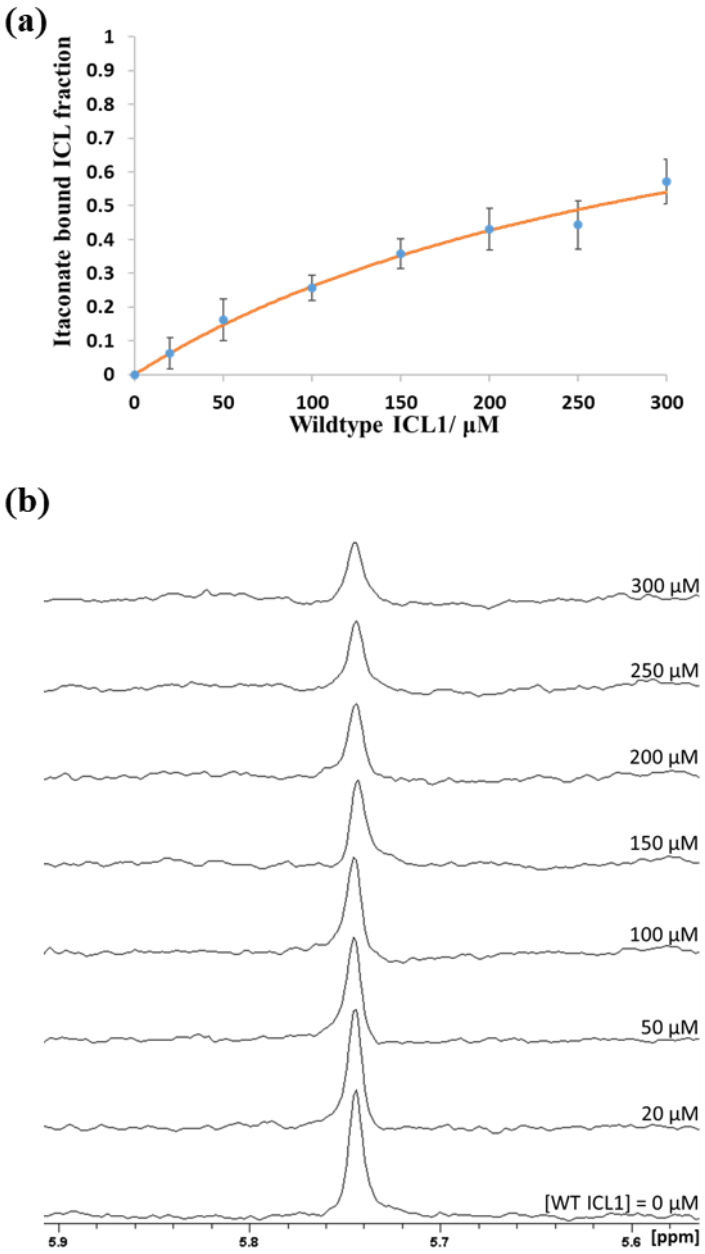

Figure S11: (a) Binding of itaconate to wildtype ICL1 in presence of glyoxylate (no Mg^{2+}). The K_D value was found to be >>500 µM. Error bars represent standard deviations from three individual experiments. **(b)** Corresponding ^1H NMR spectra. K_D measured at a fixed itaconate concentration (20 µM) and varying ICL1 concentration (0 to 300 µM). The glyoxylate concentration was 2 mM. Itaconate binding was monitored via the decrease of the itaconate alkene $=CH_2$ peak at 5.75 ppm as a function of protein concentration.

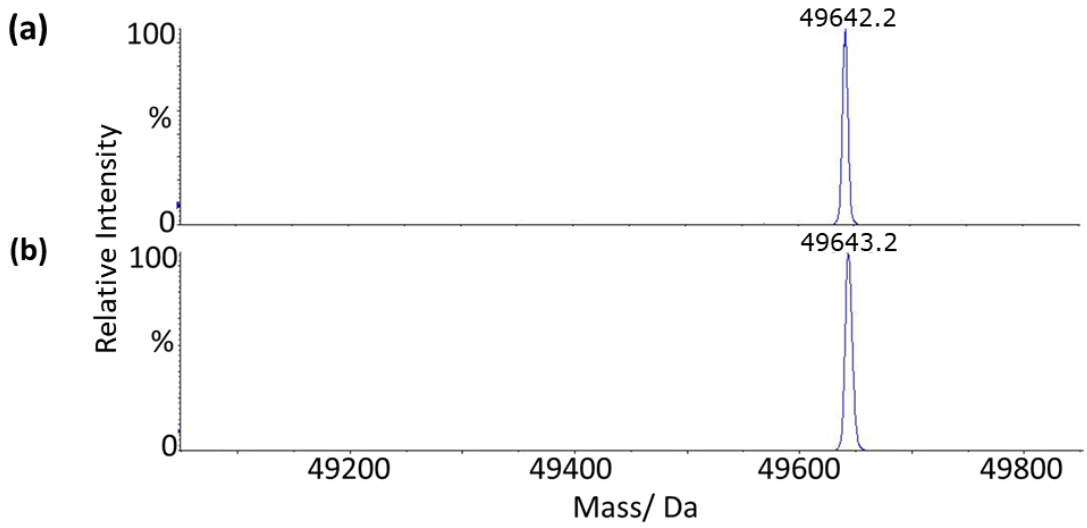

Figure S12: LC-MS analysis of **(a)** wildtype ICL1 on its own, and **(b)** wildtype ICL1 pre-incubated with itaconate and glyoxylate in the absence of Mg^{2+}. The calculated molecular weight of wildtype ICL1 is 49639.3 Da.

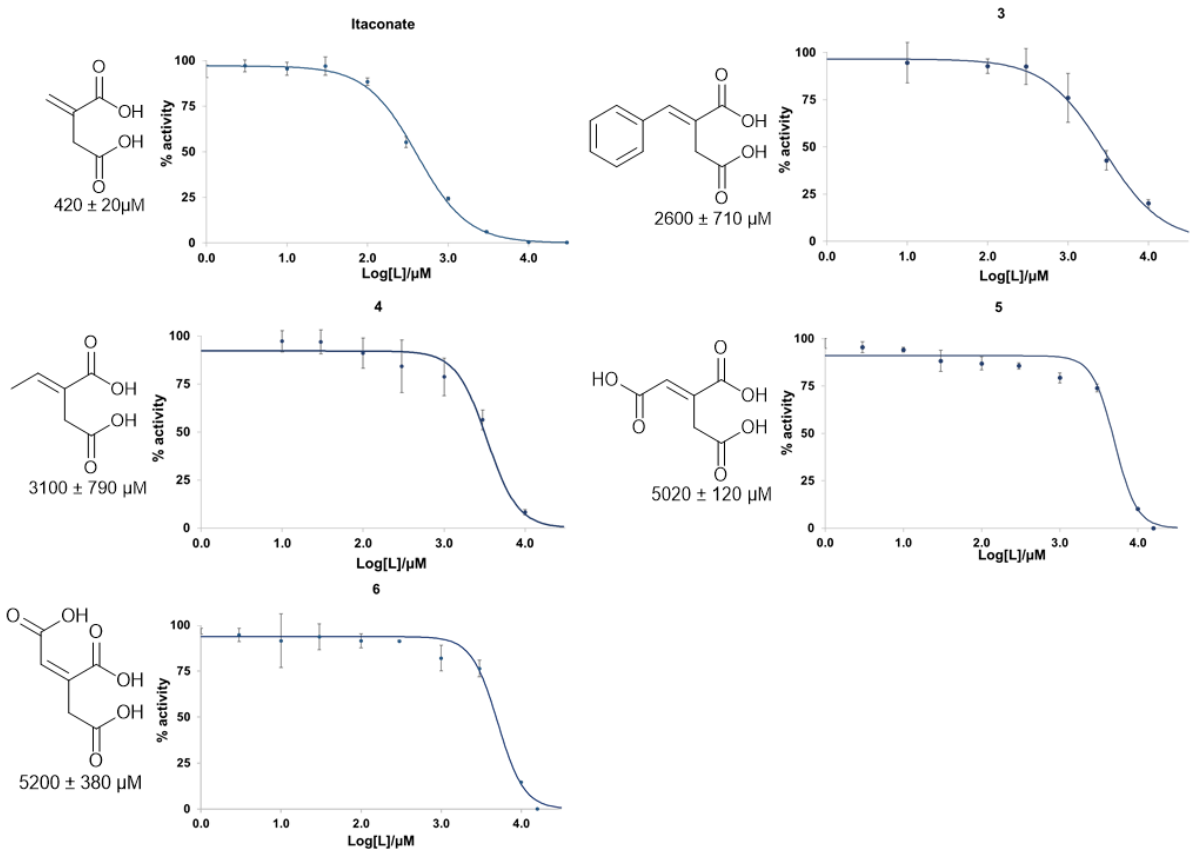

Figure S13: IC_{50} curves of itaconate analogues. Experiments contained 20 nM ICL1, 1 mM DL-isocitrate, 1 mM $MgCl_2$, 10 mM phenylhydrazine-HCl and varying concentration of itaconate analogues in 50 mM Tris (pH 7.5). Note that full inhibition was not achieved for compounds **3** and **4** due to the limited solubility of the compounds at high concentration. Errors bar represents standard deviations from four separate measurements.

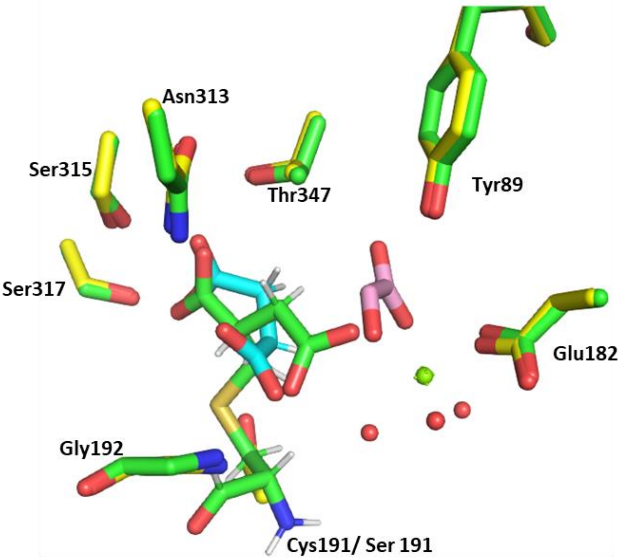

Figure S14: Structural superimposition of ICL1 active sites in the presence of different ligands. Active site residues are shown as cartoon representation for ICL1- itaconate (green), and 3-nitropropionate (cyan) and glyoxylate (pink) bound C191S ICL1 (PDB: 1F8I). Glyoxylate sits in the deeper end of the binding pocket. Arg228 is not shown for clarity. Atomic colours are as follows: oxygen, red; nitrogen, blue, hydrogen grey. Residues of 1F8I are coloured in yellow. Mg^{2+} ion is shown as a green sphere and water molecules as red spheres.

Supplementary Tables

Table S1: Amino acid and DNA sequences of C191S ICL1.

```
M  G  S  S  H  H  H  H  H  H  S  S  G  L  V  P  R  G  S  H
atgggcagcagccatcatcatcatcatcacagcagcggcctggtgccgcgcggcagccat
M  S  V  V  G  T  P  K  S  A  E  Q  I  Q  Q  E  W  D  T  N
Atgtctgtcgtcggcaccccgaagagcgcggagcagatccagcaggaatgggacacgaac
P  R  W  K  D  V  T  R  T  Y  S  A  E  D  V  V  A  L  Q  G
ccgcgctggaaggacgtcacccgcacctactccgccgaggacgtcgtcgccctccagggc
S  V  V  E  E  H  T  L  A  R  R  G  A  E  V  L  W  E  Q  L
agcgtggtcgaggagcacacgctggcccgccgcggtgcggaggtgctgtgggagcagctg
H  D  L  E  W  V  N  A  L  G  A  L  T  G  N  M  A  V  Q  Q
cacgacctcgagtgggtcaacgcgctgggcgcgctgaccggcaacatggccgtccagcag
V  R  A  G  L  K  A  I  Y  L  S  G  W  Q  V  A  G  D  A  N
gtgcgcgccggcctgaaggccatctacctgtcgggctggcaggtcgccggcgatgccaac
L  S  G  H  T  Y  P  D  Q  S  L  Y  P  A  N  S  V  P  Q  V
Ctgtccgggcacacctaccccgaccagagcctgtatcccgccaactcggtgccgcaggtg
V  R  R  I  N  N  A  L  Q  R  A  D  Q  I  A  K  I  E  G  D
gtccgccggatcaacaacgcactgcagcgcgccgaccagatcgccaagatcgagggcgat
T  S  V  E  N  W  L  A  P  I  V  A  D  G  E  A  G  F  G  G
acttcggtggagaactggctggcgccgattgtcgccgacggcgaggccggctttggcggc
A  L  N  V  Y  E  L  Q  K  A  L  I  A  A  G  V  A  G  S  H
gcgctcaacgtctacgagctgcagaaagccctgatcgccgcgggcgttgcgggttcgcac
W  E  D  Q  L  A  S  E  K  K  C  G  H  L  G  G  K  V  L  I
tgggaggaccagttggcctctgagaagaagagcggccacctgggcggcaaggtgttgatc
P  T  Q  Q  H  I  R  T  L  T  S  A  R  L  A  A  D  V  A  D
ccgacccagcagcacatccgcactttgacgtctgctcggctcgcggccgatgtggctgat
V  P  T  V  V  I  A  R  T  D  A  E  A  A  T  L  I  T  S  D
gttcccacggtggtgatcgcccgtaccgacgccgaggcggccacgctgatcacctccgac
V  D  E  R  D  Q  P  F  I  T  G  E  R  T  R  E  G  F  Y  R
gtcgacgagcgcgaccagccgttcatcaccggcgagcgcacccgggaaggcttctaccgc
T  K  N  G  I  E  P  C  I  A  R  A  K  A  Y  A  P  F  A  D
accaagaacggcatcgagccttgcatcgctcgggcgaaggcctacgccccgttcgccgac
L  I  W  M  E  T  G  T  P  D  L  E  A  A  R  Q  F  S  E  A
ttgatctggatggagaccggtaccccggacctcgaggccgcccggcagttctccgaggcg
V  K  A  E  Y  P  D  Q  M  L  A  Y  N  C  S  P  S  F  N  W
gtcaaggcggagtacccggaccagatgctggcctacaactgctcgccatcgttcaactgg
K  K  H  L  D  D  A  T  I  A  K  F  Q  K  E  L  A  A  M  G
aaaaagcacctcgacgacgccaccatcgccaagttccagaaggagctggcagccatgggc
F  K  F  Q  F  I  T  L  A  G  F  H  A  L  N  Y  S  M  F  D
ttcaagttccagttcatcacgctggccggcttccatgcgctgaactactcgatgttcgat
L  A  Y  G  Y  A  Q  N  Q  M  S  A  Y  V  E  L  Q  E  R  E
ctggcctacggctacgcccagaaccagatgagcgcgtatgtcgaactgcaggaacgcgag
F  A  A  E  E  R  G  Y  T  A  T  K  H  Q  R  E  V  G  A  G
ttcgccgccgaagaacggggctacaccgcgaccaagcaccagcgcgaggtcggcgccggc
Y  F  D  R  I  A  T  T  V  D  P  N  S  S  T  T  A  L  T  G
tacttcgaccggattgccaccaccgtggacccgaattcgtcgaccaccgcgttgaccggt
S  T  E  E  G  Q  F  H  -
tccaccgaagagggccagttccactag
```

Table S2: Data collection and processing statistics.*

	M.tb ICL1-Mg(II)-ITN
Wavelength (Å)	0.953733
Space group	$P2_12_12_1$
Cell dimensions	
a (Å)	79.31
b (Å)	133.17
c (Å)	159.32
α, β, γ (°)	90, 90, 90
Resolution range[a] (Å)	49.33- 1.55 (1.58- 1.55)
R_{merge}	0.123 (2.057)
R_{pim}	0.034 (0.56)
Observed reflections	3,362,723 (116,162)
Unique reflections	242,871 (11,809)
Multiplicity	13.8 (14.1)
Mean I/σI	11.6 (1.4)
Completeness (%)	99.7 (99)
CC(1/2)	0.999 (0.613)

*Values in parentheses are for the outermost resolution shell.

Table S3: Structure refinement statistics.

	***M.tb* ICL1-Mg(II)-ITN**
PDB code	6XPP
Resolution range (Å)	49.33- 1.55
R_{work}/R_{free} (%)	0.1584/ 0.1790
Number of atoms (non-hydrogen)	
Protein	13,251
Ligand	36
Solvent	1770
R.m.s.d. from ideality	
Bonds (Å)	0.0053
Angles (°)	1.3028
Average *B* factors (Å^2)	
Protein	21.14
Itaconate	25.43
Mg^{2+}	22.95
Waters	32.09
Ramachandran statistics (%)	
Favored	98.10
Allowed	1.90
Outliers	0.00
Molprobity score/ percentile	0.99/100th

References

[1] R. P. Bhusal, K. Patel, B. X. C. Kwai, A. Swartjes, G. Bashiri, J. Reynisson, J. Sperry, I. K. H. Leung, *MedChemComm* **2017**, *8*, 2155-2163.

[2] R. P. Bhusal, W. Jiao, B. X. C. Kwai, J. Reynisson, A. J. Collins, J. Sperry, G. Bashiri, I. K. H. Leung, *Nature Communications* **2019**, *10*, 4639.

[3] Valjakka J., Hemminki A., T. K. Teerinen T., R. J., *Acta Crystallogr.* **2000**, *56*, 218-221.

[4] T. M. McPhillips, S. E. McPhillips, H.-J. Chiu, A. E. Cohen, A. M. Deacon, P. J. Ellis, E. Garman, A. Gonzalez, N. K. Sauter, R. P. Phizackerley, S. M. Soltis, P. Kuhn, *Journal of Synchrotron Radiation* **2002**, *9*, 401-406.

[5] W. Kabsch, *Acta Crystallographica* **2010**, *D66*, 125-132.

[6] P. Evans, *Acta Crystallographica* **2006**, *D62*, 72-86.

[7] A. J. McCoy, R. W. Grosse-Kunstleve, P. D. Adams, M. D. Winn, L. C. Storoni, R. J. Read, *J. Appl. Crystallogr* **2007**, *40*, 658-674.

[8] V. Sharma, S. Sharma, K. H. zu Bentrup, J. D. McKinney, D. G. Russell, W. R. Jacobs, J. C. Sacchettini, *Nature Structural Biology* **2000**, *7*, 663-668.

[9] P. Emsley, K. Cowtan, *Acta Crystallographica* **2004**, *D60*, 2126-2132.

[10] G. N. Murshudov, P. Skubák, A. A. Lebedev, N. S. Pannu, R. A. Steiner, R. A. Nicholls, M. D. Winn, F. Long, A. A. Vagin, *Acta Crystallographica* **2011**, *D67*, 355-367.

[11] R. A. Nicholls, *Acta Crystallographica* **2017**, *D73*, 158-170.

[12] A. W. Schüttelkopf, D. M. F. van Aalten, *Acta Crystallographica* **2004**, *D60*, 1355-1363.

[13] R. P. Joosten, F. Long, G. N. Murshudovb, A. Perrakisa, *IUCrJ* **2014**, *1*, 213-2220.

[14] I. W. Davis, A. Leaver-Fay, V. B. Chen, J. N. Block, G. J. Kapral, X. Wang, L. W. Murray, W. B. Arendall, III, J. Snoeyink, J. S. Richardson, D. C. Richardson, *Nucleic Acids Research* **2007**, *35*, W375-W383.

[15] T. V. Pham, A. S. Murkin, M. M. Moynihan, L. Harris, P. C. Tyler, N. Shetty, J. C. Sacchettini, H.-l. Huang, T. D. Meek, *Proceedings of the National Academy of Sciences* **2017**, *114*, 7617.

[16] D. Malferrari, N. Armenise, S. Decesari, P. Galletti, E. Tagliavini, *ACS Sustainable Chemistry & Engineering* **2015**, *3*, 1579-1588.

[17] R. Ballini, A. Rinaldi, *Tetrahedron Letters* **1994**, *35*, 9247-9250.

[18] Y. Wang, R. Mowla, S. Ji, L. Guo, M. A. De Barros Lopes, C. Jin, D. Song, S. Ma, H. Venter, *European Journal of Medicinal Chemistry* **2018**, *143*, 699-709.

[19] R. Ballini, G. Bosica, A. Palmieri, M. Petrini, C. Pierantozzi, *Tetrahedron* **2003**, *59*, 7283-7289.

[20] R. P. Bhusal, G. Bashiri, B. X. C. Kwai, J. Sperry, I. K. H. Leung, *Drug Discovery Today* **2017**, *22*, 1008-1016.

[21] M. M. Moynihan, A. S. Murkin, *Biochemistry* **2014**, *53*, 178-187.

[22] J. C. Aon, R. J. Caimi, A. H. Taylor, Q. Lu, F. Oluboyede, J. Dally, M. D. Kessler, J. J. Kerrigan, T. S. Lewis, L. A. Wysocki, P. S. Patel, *Appl Environ Microbiol* **2008**, *74*, 950-958.